Inhibition of phosphodiesterase - 10A by Papaverine protects human cortical neurons from quinolinic acid induced oxidative stress and synaptic proteins alterations

Abid Bhat[1,2], Vanessa Tan[2], Benjamin Heng[2], Musthafa M. Essa[3,4,], Saravana B. Chidambaram[1,5*],Gilles J. Guillemin[2*]

1. Department of Pharmacology, JSS College of Pharmacy, JSS Academy of Higher Education & Research, Sri Shivarathreeshwara Nagar, Mysuru, Karnataka 570015, India
2. Neuroinflammation Group, Faculty of Medicine, Health and Human Sciences, Macquarie University, Sydney, NSW, Australia.
3. Department of Food Science and Nutrition, CAMS, Sultan Qaboos University, Muscat, Oman
4. Ageing and Dementia Research Group, Sultan Qaboos University, Muscat, Oman
5. Centre for Experimental Pharmacology and Toxicology, Central Animal Facility, JSS Academy of Higher Education & Research, Mysuru, India

For correspondence

Prof Gilles J. Guillemin

Head of the Neuroinflammation group

Faculty of Medicine and Health Sciences

Macquarie University NSW, 2109 Australia

Phone: 61 (02) 9850 2727.Email:gilles.guillemin@mq.edu.au

&

Prof. Saravana Babu Chidambaram

Associate Professor, Department of Pharmacology

JSS College of Pharmacy & Coordinator, CPT, JSS AHER,

Mysuru, Karnataka 570015, India

Mob: +91-904222227. Email: babupublications@gmail.com

Abstract

Phosphodiesterase-10A (PDE10A) hydrolyse the secondary messengers cGMP and cAMP which play critical role in neurodevelopment and brain functions. PDE10A is linked to progression of neurodegenerative diseases like Alzheimer's, Parkinson's, Huntington's diseases etc and a critical role in cognitive functions. The present study was undertaken to determine the possible neuroprotective effects and the associated mechanism of papaverine (PAP) against quinolinic acid (QUIN) induced excitotoxicity using human primary cortical neurons. Cytotoxicity potential of PAP was analysed using MTS assay. Reactive oxygen species (ROS) and mitochondrial membrane potential were measured by DCF-DA and JC10 staining, respectively. Caspase 3/7 and cAMP levels using ELISA kits. Effect of PAP on the CREB, BNDF and synaptic proteins such as SAP-97, synaptophysin, synapsin-I, PSD-95 expression was analysed by Western blotting technique. Pre-treatment with PAP increased intracellular cAMP and nicotinamide adenine dinucleotide (NAD^+) levels, restored mitochondrial membrane potential ($\Delta\Psi m$), and decreased ROS and caspase3/7 content in QUIN exposed neurons. PAP up-regulated CREB and BDNF, and synaptic proteins expression. In summary, these data indicate that PDE10A involves in QUIN mediated neurotoxicity and its inhibition can elicit neuroprotection by reducing the oxidative stress and protecting synaptic proteins via upregulation of cAMP signalling cascade.

Keywords: Phosphodiesterase-10A, cAMP, papaverine, quinolinic acid, oxidative stress, synaptic proteins

Introduction

Phosphodiestrase-10A (PDE10A) is a key enzyme involved in hydrolysis of intracellular second messengers cyclic adenosine monophosphate (cAMP) and cyclic guanosine monophosphate (cGMP) in brain (Niccolini et al., 2015). cAMP activates protein kinase A (PKA), resulting in the phosphorylation of the transcription factor cAMP response element binding protein (CREB) which in turn induces the protein expression of brain-derived neurotrophic factor (BDNF) and put together these protein regulate a wide range of biological functions, such as synaptic plasticity, learning and memory etc. (Kowiański et al., 2018). Imbalance in cAMP level is implicated in the various neurodegenerative diseases (Roush et al., 2020). Dysregulation of tryptophan metabolism leads to the production of kynurenine metabolites. Quinolinic acid (QUIN) is a neuro- and gliotoxic metabolite produced in

kynurenine pathway (KP) (Guillemin, 2012). QUIN causes neurotoxicity by overactivation of N-methyl-D-aspartate (NMDA) receptors and by forming a coordination complex with iron and copper resulting in excessive intracellular Ca^{2+} overload (Chen et al., 2010). It triggers oxidative stress by increasing neuronal nitric oxide synthase (nNOS) and lipid peroxidation (Braidy et al., 2009a). It also impairs mitochondrial oxygen consumption and causes mitochondrial complex (I, II, III and IV) dysfunction (Mishra and Kumar, 2014). Higher levels of QUIN have been found in Alzheimer's disease (AD) (G. J. Guillemin et al., 2005), Parkinson's disease (PD) (Zinger et al., 2011), multiple sclerosis (MS) (Lim et al., 2017; Sundaram et al., 2014), Huntington's disease (HD) (Sumathi et al., 2018). QUIN exposure increases poly (ADP-ribose) polymerase (PARP) activity, depletes NAD^+ and adenosine triphosphate (ATP) production in human primary neurons (Braidy et al., 2010). Depletion of ATP causes mitochondrial membrane potential ($\Delta\psi m$) collapse in turn the release of cytochrome c (cyt c) and neuronal death (Cao et al., 2011). QUIN intoxication is shown to decreases the synapse number in hippocampus region of the rat via down-regulatingexpression of synaptic proteins such as PSD-95 and reduced phosphorylation of CREB and BNDF expression in rats (Rahman et al., 2018).

Oxidative stress and excitotoxicity suppresses expression of synaptic markers such as synapsin I, synaptophysin, BDNF, calcium□calmodulin dependent protein kinases II and Calcineurin A which hinders brain development and function (Ansari et al., 2008a). PDE10A is an isoenzyme distributed in various brain regions (cerebellum, thalamus, hippocampus, and spinal cord etc); but it is highly expressed in frontal cortex (Heckman et al., 2016). Synaptic density increases in cortical regions after birth in humans (Huttenlocher and Dabholkar, 1997). Interestingly, synaptic proteins are highly expressed in the cortical region and play a vital role in the cortical development (Azir et al., 2018; Valtschanoff et al., 2000). Interaction of pre and postsynaptic proteins facilitate synapse development, communication, long term potentiation and memory formation (Abraham et al., 2019). Alterations in the cortical synaptic proteome is a prominent pathological feature in AD (Counts et al., 2006). Cortical neurons are more vulnerable to ROS attacks which affect synaptic proteins as well (Ansari et al., 2008b). Studies in knockout mice suggests that PDE10A is involved in regulating basal ganglia circuit which governs motor, emotional, and cognitive functions, maintains the energy homeostasis and has a thermoregulatory role (Giampà et al., 2010; Hankir et al., 2016; Siuciak et al., 2006). Its involvment in in neurological disorders such as schizophrenia (Persson et al., 2020) and HD (Giralt et al., 2013) is well documented. Papaverine (PAP), a

PDE10A isoenzyme inhibitor, is an major alkaloid obtained from the opium latex of *Papaver somniferum*, family: Papaveraceae (Han et al., 2010) (Fig.1). PAP is clinically used as a vasodilator and smooth muscle relaxant which mediates its action via cAMP (Kim et al., 2014; Wilson and White, 1986). Phosphodiestrase (PDE) inhibitors are being increasingly considered as therapeutic class for neurological disorders (Bhat et al., 2020). PAP is a potent PDE10A inhibitor with an EC50 value of 36 nM, devoid of any narcotic properties and with lesser side effects as compared to PDE4 inhibitors (Boswell-Smith et al., 2006; Heckman et al., 2016). Understaning the physiological role of PDE10A and advanatges of its inhibitor particualry in brain fucntions, in the present study we investigated the potential effects of PAP against QUIN induced neurotoxicity in human primary cortical neurons. We investigated the effects of PAP on oxidative stress, NAD+/NADH production, Caspase activity, cAMP signaling cascade and synaptic proteins expression in QUIN exposed human neurons.

Materials and Methods

Reagents and antibodies

Papaverine, quinolinic acid, 2′,7′-dichlorofluorescin diacetate (DCFDA) were purchased from Sigma Aldrich (Castle-Hill, Australia). CellTiter 96® Aqueous One Solution cell proliferation assay kit and ApoTox-Glo™ Triplex Assay kit was obtained from Promega, Australia. JC-10 staining kit was obtained from AAT Bioquest, Australia. NAD/NADH Assay Kit, cAMP Elisa kit (ab234585), Rabbit Anti-PSD95 (ab18258), Rabbit Anti-SAP97 (ab3437), Mouse Anti-Synaptophysin (ab8049), Rabbit Anti-BDNF (ab108319) were procured from Abcam, USA. Rabbit Anti-CREB, Rabbit Anti-Synapsin I was obtained from Sigma Aldrich, USA. All other reagents and chemicals used were of analytical grade.

Primary cortical neuronal culture

Human neuronal cell culture was generated from the 17- to 20-week-old foetal brain tissue collected after therapeutic termination following written informed consent obtained from the participant. Approval for this study was taken from Human Research Ethics Committee of Macquarie University **(Ethics approval: 5201300330).** The cortical neuronal cultures were prepared and maintained according to the method described by Guillemin et al. (2005b). Cells were plated in 96 well and 12-well culture plates coated with Matrigel (1/20 in Neurobasal) and maintained in Neurobasal medium supplemented with 1% B-27 supplement, 1% Glutamax, 1% antibiotic/antifungal (Penicillin G 200 IU/mL, streptomycin sulphate 200

µg/mL), 0.5% HEPES buffer, and 0.5% glucose. The cells were maintained at 37°C in a humidified atmosphere containing 95% air/5% CO_2 (Guillemin et al., 2007).

Cell viability assay

Cell viability of papaverine was evaluated using CellTiter 96® AQueous One Solution Reagent (Promega) based on mitochondrial dehydrogenase activity. Neuronal cells were seeded in Matrigel (1/20 in Neurobasal) coated 96 well plate and incubated with a range of PAP concentrations (0.5, 1, 2, 5, 10, 20 µM) at 37°C for 72 hours. Twenty microliters of [3-(4,5-dimethylthiazol-2-yl)-5-(3-carboxymethoxyphenyl)-2-(4-sulfophenyl)-2H-tetrazolium (MTS) solution was added to each well. Absorbance was read at 490 nm in a microplate reader (PHERAstar FS) at 24, 48 and 72 hours after PAP exposure.

Treatment protocol

Human primary neurons were pre-treated for 24 h with papaverine (2 and 5 µM; doses were fixed based on cytotoxicity assay results) followed by 48 hours exposure with QUIN (2 µM) at 37°C.

Reactive Oxygen Species detection using 2-7-Dichlorofluorescin Diacetate Assay

Intracellular reactive oxygen species levels in primary human neurons was estimated using 2-,7-dichlorofluorescin (DCF)-DA assay. (Kim et al., 2012). After completing the treatment, cells were washed with ice cold phosphate-buffered saline (PBS). DCF-DA (20 µM) was added and incubated for 30 minutes. Fluorescence intensity was measured using a microplate reader (PHERAstar FS, BMG Labtech) (excitation wavelength of 495 nm and emission wavelength of 515 nm). ROS production was calculated as a percentage of the control.

Mitochondrial membrane potential (ΔΨm) assessment

Mitochondrial membrane potential was determined by using highly sensitive JC-10 (tetraethyl benzimidazolylcarbocyanide iodine) staining as per the manufacturer's instructions (Li et al., 2016). The accumulation of the JC-10 dye is proportional to the mitochondrial membrane potential. JC-10 gives green and red to orange fluorescence in low and high $\Delta\Psi m$, respectively. Following the pre-treatment with PAP, cells were washed with ice cold PBS. 100 µL of JC-10 stain (30 µM) added and incubated for 20 minutes. JC-10 staining in the culture media was removed and 100 µL of HEPES buffer was added. The

158 change in fluorescence intensity was measured using microplate reader (PHERAstar FS) at
159 Ex/Em = 490/525 nm and 540/590nm. The shift from green to red indicates depolarisation.

160 **Measurement of caspase 3/7 activity**

161 Caspase 3/7 activity in primary neuronal cells was measured using ApoTox-Glo Triplex
162 Assay kit (Promega, Madison, WI, USA) as per the manufacture's instruction. Cells were
163 treated with PAP and QUIN as mentioned in the treatment protocol. 50 µL of caspase Glo 3/7
164 reagent was added to each well and incubated for 2 hours at room temperature with constant
165 shaking. Caspase 3/7 activity was analysed by measuring luminescence using a microplate
166 reader (PHERAstar FS).
167
168

169 **Estimation of intracellular NAD^+/NADH levels**

170 Intracellular NAD^+/NADH ratio were measured using NAD/NADH Assay Kit (Abcam, Inc.,
171 Cambridge, MA, USA) as per the instructions (Ren et al., 2010, p. 2). Cells were washed
172 with ice cold PBS following the completion of treatment protocol. The cells were lysed with
173 400 µL of NAD^+/NADH extraction buffer containing a cocktail of protease inhibitor (Roche
174 Diagnostic, Castle Hill, NSW, Australia) and centrifuged at 10000×g for 5 min at 4°C. To
175 measure NAD^+, 200 µL aliquot of cell lysate was heat quenched at 60°C for 30 min. An
176 equal volume of NAD^+/NADH reaction mixture was added to each well with cell lysate,
177 incubated at room temperature for 60 min, and absorbance was read at 450 nm using a
178 microplate reader (PHERAstar FS). The concentration of NAD^+ or NADH was calculated
179 using a standard calibration curve.

180 **Measurement of cAMP concentration**

181 Cells were seeded in 12 well plate and were pre-treated with vehicle or PAP (2 and 5 µM) for
182 24 hours and then exposed to QUIN (2 µM) for 48 hours. At the end of the treatment protocol,
183 cells were washed with ice cold PBS and lysed using 0.1 M HCl for 20 minutes and
184 centrifuged for 10 minutes. Cell lysate was collected, and cAMP concentration was measured
185 using a direct immunoassay kit (Abcam, MA) following the manufacturer's instruction. In
186 brief, standards and samples were added to wells coated with an IgG antibody. A cAMP
187 conjugated to alkaline phosphatase was then added, followed by a rabbit polyclonal antibody
188 against cAMP. The antibody binds to cAMP in the sample or to the conjugate in a

competitive manner. The plate was washed, leaving only bound cAMP. para-Nitrophenyl phosphate (pNpp) substrate solution was added and produced a yellow color when catalyzed by the alkaline phosphatase on the cAMP conjugate. The stop solution was then added, and the yellow color was read at 405 nm using a microplate reader (PHERAstar FS), and concentration of cAMP was calculated using a standard calibration curve.

Western blot analysis

Cells were lysed with radioimmunoprecipitation assay (RIPA) buffer (50 mM Tris, pH 7.4, 150 mM NaCl, 1% NP-40, 5 mM EDTA, 0.5% sodium deoxycholate, 0.1% SDS, 50 nMNaF, 1 mM sodium vanadate) containing a cocktail of protease inhibitor (Roche Diagnostic, Castle Hill, NSW, Australia). Total protein concentration was determined by BCA protein assay (Bio-Rad Laboratories, Hercules,CA, USA), cell lysate samples were aliquoted and stored at -80^{o}C till used. Proteins (20 µg) were separated by using 12% bis-tris -SDS-PAGE (NuPAGE, Invitrogen, Carlsbad CA, USA) by electrophoresis. Resolved proteins in the gels were transferred onto nitrocellulose membranes (Biorad) and electroblotted. Membranes were blocked with 5% non-fat skimmed milk in Tris-Buffered Saline and Tween 20 (TBST) for 1 hour followed by overnight incubation with the primary antibodies CREB (1:1000), BDNF (1:1000), PSD-95 (1:1000), Synapsin (1:1000), Synaptophysin (1:1000), SAP 97 (1:1000) at 4^{o}C. The membranes were rinsed with TBST (3 washings for 10 minutes), incubated with the secondary antibodies (HRP conjugated anti-mouse or anti-rabbit IgG) for 1 h at room temperature followed by 3 washings for 10 mins with TBST. The bands were visualised by Odyssey Infrared Imaging System; Li-Cor, Lincoln, NE

Statistical analysis

Data were presented as mean ±SEM. Group mean differences were analysed using one-way ANOVA test followed by Tukey's multiple comparison test as post hoc test. Results were analysed using GraphPad Prism version 7.04 with probability value of $p \leq 0.05$ considered as significant.

Results

Cell viability

Cell viability was tested using CellTiter 96® AQueous One Solution Reagent (Promega) after 24-, 48 and 72-hour treatment with papaverine at concentrations 0.5, 1, 2, 5, 10 and 20 µM. **(Fig.2).** We did not observe time or concentration dependent neuronal death in cell viability assay

Papaverine reduces QUIN induced reactive oxygen species (ROS) generation in human cortical neurons

QUIN exposed neurons showed significant (p <0.01) increase in ROS production compared to vehicle treated cortical neurons. Pre-treatment with PAP reduced ROS production in QUIN intoxicated neurons. But a significant (p <0.01) decrease in ROS production was observed at 5 µM concentration **(Fig. 3)**. This shows that PAP has the potential to reduce oxidative stress.

Papaverine restores mitochondrial membrane potential (ΔΨm) in QUIN exposed human neurons

Mitochondrial oxidative stress and ΔΨm are involved in the neurodegeneration. Amelioration of mitochondrial dysfunction is proposed as an effective way for slowing down the progression of neurodegeneration (Wu et al., 2019). Increased production of ROS affects mitochondrial structure and function, we assessed ΔΨm by using JC10 staining. Mitochondrial depolarization results in dye release and unquenching, increasing the fluorescence signal is proportional to ΔΨm values. In QUIN exposed human neurons we found that fluorescence intensity increased significantly (p < 0.01) when compared with vehicle treated neurons, indicating increased mitochondrial depolarisation. Pre-treatment with PAP decreased mitochondrial depolarization in QUIN intoxicated neurons with a significant (p <0.05) protection recorded at 5µM **(Fig. 4).**

Papaverine suppressed QUIN induced caspase 3/7 activity in human neurons

Neurons primarily use the intrinsic apoptotic pathway to undergo cell death and role of caspase-3 and caspase 7 in progression of neurodegeneration is well studied using knockout mouse model (D'Amelio et al., 2010). Increase in the oxidative stress elicits neurodegeneration by activating the early apoptosis cascade (Dos Santos et al., 2018). We found that QUIN significantly (p < 0.01) increased caspase3/7 activity in neurons when compared to vehicle treated cells. Pre-treatment with papaverine reduced QUIN induced caspase 3/7 activity with a significant (p < 0.01) decrease at 5 µM concentration when compared with QUIN alone exposed cells (**Fig.5).**

Papaverine increases intracellular NAD^+/NADH level in human neurons

We also investigated the effects of PAP on NAD/NADH content in QUIN treated cells. Human neurons exposed to QUIN showed significant ($p < 0.01$) decrease in intracellular NAD^+/NADH content when compared with the vehicle treated cells. Papaverine pre-treatment showed dose dependent increase in NAD^+/NADH content and a significant ($p < 0.01$) increase was found at 5 µM when compared with QUIN exposed human neurons **(Fig. 6).**

Papaverine increases intracellular cAMP content in QUIN exposed human neurons

Next, we investigated the effects of PAP on cAMP content in human neurons using ELISA kit. QUIN exposed neurons were found to have a significant ($p < 0.05$) decrease in cAMP levels as compared to vehicle treated neurons. Pre-treatment with PAP increased the cAMP levels when compared with QUIN exposed neurons with a significant ($p < 0.01$) increase at 5 µM concentration **(Fig.7).**

Papaverine upregulated CREB/ BDNF expression in primary human neurons

Further we investigated the effects of PAP on the expression of CREB and BDNF in QUIN exposed human cortical neurons. CREB is an important cellular transcription factor regulating the expression of neurotrophic factors such as BDNF are important for synaptic plasticity and memory (Wang et al., 2018). QUIN was shown to significantly ($p < 0.05$) reduce the expression of CREB in human neurons. Pre-treatment with papaverine significantly increased ($p <0.05$) the expression of CREB in human neurons **(Fig.8A).** Brain-derived neurotrophic factor (BDNF) is reported to play an important role in the survival of neurons (Miranda et al., 2019). A significant decrease ($p < 0.05$) in BDNF expression was found in QUIN exposed human neurons. Pre-treatment with papaverine significantly ($p < 0.01$) reversed the QUIN induced decline in BDNF expression in human neurons as compared to QUIN exposed cells **(Fig.8B)**.

Papaverine increased the expression of synaptic associated proteins like Synapsin-I, Synaptophysin, PSD-95 and SAP-97

Next, we investigated the effects of PAP against QUIN mediated synaptic damage in human neurons. QUIN exposure significantly reduced the expression of Synapsin I ($p < 0.05$), synaptophysin ($p < 0.01$), PSD-95 ($p < 0.01$) and SAP-97 ($p < 0.05$) in human neurons. Pre-treatment with PAP significantly upregulated the expression of Synapsin I ($p < 0.01$),

281 synaptophysin ($p < 0.01$), PSD-95 ($p < 0.01$) and SAP-97 ($p < 0.01$) when compared with
282 QUIN exposed neurons **(Fig. 9).** Taken together, these results indicate that inhibition of
283 PDE10A with papaverine was enough to induce both presynaptic and postsynaptic
284 remodelling and instigate the expression of synapsis associated proteins in QUIN exposed
285 human neurons.

286 **Discussion**

287 The present study is the first of its kind to show the protective effects of papaverine against
288 QUIN induced excitotoxicity in human neurons. Our results showed that PAP alleviates
289 oxidative stress by upregulating cAMP and enhances the expression of synaptic proteins.
290 PDE10A is highly expressed in the hippocampus and cortex which are highly vulnerable to
291 excitotoxicity (Heckman et al., 2016). PDE10A plays a pivotal role in these neurons as it
292 regulate cAMP cascade and its inhibition is shown to activate and phosphorylate CREB and
293 other neurotrophic factors (Steffan et al., 2000). Increased expression of PDE10A precipitates
294 NMDA receptors and increased dopamine D_1- and D_2 receptor activity which alters
295 cognitive and motor functions by disrupting the integration of information from cortical
296 projections (Smith et al., 2013). Several studies have shown that PDE10A is implicated in the
297 progression of neurodegenerative diseases such as HD (Cardinale and Fusco, 2018; Harada et
298 al., 2017), PD (García et al., 2014; Lee et al., 2019a), MS (Suzumura et al., 1999)
299 schizophrenia (Schmidt et al., 2008) and cognitive dysfunctions (Rodefer et al., 2012) which
300 is due to overexcitation of NMDA receptors and disruption of mitochondrial bioenergetics
301 (Bading, 2017).

302 Oxidative stress causes destruction of genetic materials, lipids and proteins (Birben et al.,
303 2012) and also linked to the pathogenesis of many neurodegenerative diseases (Islam, 2017).
304 Recenty we compiled the data that sleep deprivation alters tryptophan metabolism and the
305 neurotoxic KP metabolites produced impairs the cognitive functions **(**Abid, 2020). In this
306 study we used QUIN to induce oxidative stress in human neurons and observed that PAP, a
307 cAMP specific PDE10A inhibitor, has promising neuroprotective effects via improving
308 cAMP signalling and synaptic proteins expression. QUIN increases PARP activity, depletes
309 NAD^+ (Braidy et al., 2009b), ATP production and activates apoptotic cascade resulting in
310 neuronal death (Gilles J Guillemin et al., 2005). Inhibition of PDE class of enzymes have
311 been found to reduce the apoptosis in neuronal cells (Mizuno et al., 2004). In the present
312 study QUIN exposure induced ROS production, caused mitochondrial membrane

depolarization, increased Caspase3/7 activity, and reduced NAD^+/NADH content in human primary neurons. Papaverine administration have been found to reduced Caspase-3 expression (Yurtsever Kum et al., 2018) and lipid peroxidation in rats (Chandra et al., 2000). Papaverine is reported to restore mitochondrial respiration (Benej et al., 2018) by inhibiting ROS production via supressing the expression of p47phox and improving Nrf2/ARE signalling cascade in PD mouse model (Lee et al., 2019b). Consistently, in the present study, we also observed a decrease in the production of ROS, restoration of mitochondrial membrane potential, decrease in caspase3/7 activity and increased production of NAD^+ in human neurons treated with papaverine, which reveals the crucial role of PDE10A on oxidative stress and apoptosis. cAMP signalling cascade contributes in reducing inflammation and oxidative stress (Jung et al., 2010). Upregulation of PKA/CREB is closely linked with the ROS neutralising, reducing neuroinflammation and increasing mitochondrial biogenesis (Fernandez-Marcos and Auwerx, 2011). PAP improved cognitive function in HD mice by upregulating the expression of cAMP/CREB in hippocampal region (Giralt et al., 2013). It is reported to increase the expression of neurotrophic factors like BDNF and GNDF which are necessary for the neuronal survival (Lee et al., 2019b). Increased expression of BDNF facilitates long term potentiation and enhances memory consolidation in mice (Radiske et al., 2017). Earlier we showed that PDE4 inhibition upregulates CREB/BDNF expression in renovascular hypertensive rats (Jabaris et al., 2015). Similarly, PDE10A inhibition with PAP shown to exert neuroprotective effect by supressing microglial activation via nuclear factor kappa-light-chain-enhancer of activated B cells (NF-κB) signaling pathway and proinflammatory mediators and upregulates peroxisome proliferator-activated receptor gamma (PPARγ) signaling in mice (Dang et al., 2016; Lee et al., 2019b).

The current study adds evidence that PDE10A inhibition also increases cAMP/CREB and BDNF expression in the QUIN intoxicated human neurons. Further, cAMP is shown to influences the expression of synaptic proteins which are necessary for synaptic transmission and release of neurotransmitters (Leenders and Sheng, 2005). Activation of cAMP/PKA/CREB cascade enhances synaptic transmission in hippocampal neurons (Leenders and Sheng, 2005). Furthermore, BDNF upregulates the expression of presynaptic and postsynaptic proteins such as PSD-95, SAP-97, synaptophysin in cortical neurons of Sprague-Dawley rats (Jourdi and Kabbaj, 2013). We have also recorded a significant increase in the expression of presynaptic and postsynaptic proteins like SAP-97, synaptophysin, synapsin-I and PSD-95 with PAP pre-treatment in QUIN exposed human cortical neurons.

Thus it can be inferred that PAP produces neuroprotection by upregulating cAMP signalling cascade which combats the oxidative stress and synaptic dysfunction. Further in vivo studies are in progress in our lab to study the effects of papaverine on synaptic proteins expression and cognition in sleep deprived mice, wherein altered kynurenine metabolism and increased QUIN level produces neurotoxicity.

Conclusion

The present study reports the neuroprotective effects of papaverine, a PDE10A inhibitor, against quinolinic acid induced excitotoxicity in human neurons. Our study suggests that upregulation of cAMP cascade by papaverine plays a key role in reducing oxidative stress and increasing the expression of synaptic proteins. Therefore, papaverine may be considered a promising therapeutic candidate for further studies aiming to improve synaptic function in neurodegenerative diseases.

Acknowledgment

Mr. Abid Bhat is supported by the IBRO-APRC Exchange Fellowships program, Macquarie University and Senior Research Fellowship from the Indian Council of Medical Research (ICMR, New Delhi, India). Prof Guillemin is supported by the National Health Medical Research Council (NHMRC), the Australian Research Council (ARC), the Hanbury Foundation, the Mason Foundation and Macquarie University.

Conflicts of interest

Authors declare no conflicts of interest.

Informed Consent

Written informed consent was obtained from the parents (5201300330).

Abbreviations

AD: Alzheimer's diseases; ALS: Amyotrophic lateral sclerosis; ANOVA: Analysis of variance; Aβ: Amyloid beta; ARE: Antioxidant response element; ATP: Adenosine triphosphate; BDNF: Brain-derived neurotrophic factor; cAMP: Cyclic adenosine monophosphate; cGMP: Cyclic guanosine monophosphate; CREB: cAMP response element-binding protein; Cyt c: Cytochrome c; DCFDA: 2□,7□-Dichlorofluorescin Diacetate; EDTA: Ethylenediaminetetraacetic acid; HEPES: 4-(2-hydroxyethyl)-1-piperazineethanesulfonic acid; HD: Huntington's disease; JC-10:5,5,6,6'-tetrachloro-1,1',3,3' tetraethylbenzimi-dazoylcarbocyanine iodide; KP: Kynurenine pathway; MS: Multiple sclerosis; MTS: 3-(4,5-

dimethylthiazol-2-yl)-2,5-diphenyltetrazolium bromide; NAD: Nicotinamide adenine dinucleotide; NMDA: N-methyl-D-aspartate; NF-Kb: Nuclear factor kappa-light-chain-enhancer of activated B cells; nNOS: Neuronal nitric oxide synthase; Nrf2: Nuclear erythroid 2-related factor 2; PAP: Papaverine; PARP: Poly (ADP-ribose) polymerase; PBS: Phosphate-buffered saline; PD: Parkinson's disease; PDE: Phosphodiesterase; PDE10A: Phosphodiesterase-10A; PKA: Protein kinase A; pNpp: para-Nitrophenyl phosphate; PPARγ: Peroxisome proliferator-activated receptor gamma; PSD-95: Post synaptic density protein-95; QUIN: Quinolinic acid; RIPA: Radioimmunoprecipitation assay; ROF: Roflumilast; ROS: Reactive oxygen species; SAP 97: Synapse-associated protein 97; SDS: Sodium dodecyl sulphate; SYN1: Synapsin- I; TBST; Tris-Buffered Saline and Tween 20; $\Delta\Psi m$: mitochondrial membrane potential

References

Abraham, W.C., Jones, O.D., Glanzman, D.L., 2019. Is plasticity of synapses the mechanism of long-term memory storage? Npj Sci. Learn. 4, 1–10. https://doi.org/10.1038/s41539-019-0048-y

Ansari, M.A., Roberts, K.N., Scheff, S.W., 2008a. A time course of contusion-induced oxidative stress and synaptic proteins in cortex in a rat model of TBI. J. Neurotrauma 25, 513–526. https://doi.org/10.1089/neu.2007.0451

Ansari, M.A., Roberts, K.N., Scheff, S.W., 2008b. Oxidative stress and modification of synaptic proteins in hippocampus after traumatic brain injury. Free Radic. Biol. Med. 45, 443–452. https://doi.org/10.1016/j.freeradbiomed.2008.04.038

Bading, H., 2017. Therapeutic targeting of the pathological triad of extrasynaptic NMDA receptor signaling in neurodegenerations. J. Exp. Med. 214, 569–578. https://doi.org/10.1084/jem.20161673

Benej, M., Hong, X., Vibhute, S., Scott, S., Wu, J., Graves, E., Le, Q.-T., Koong, A.C., Giaccia, A.J., Yu, B., Chen, C.-S., Papandreou, I., Denko, N.C., 2018. Papaverine and its derivatives radiosensitize solid tumors by inhibiting mitochondrial metabolism. Proc. Natl. Acad. Sci. U. S. A. 115, 10756–10761. https://doi.org/10.1073/pnas.1808945115

Bhat, A., Ray, B., Mahalakshmi, A.M., Tuladhar, S., Nandakumar, D., Srinivasan, M., Essa, M.M., Chidambaram, S.B., Guillemin, G.J., Sakharkar, M.K., 2020. Phosphodiesterase-4 enzyme as a therapeutic target in neurological disorders. Pharmacol. Res. 105078. https://doi.org/10.1016/j.phrs.2020.105078

Birben, E., Sahiner, U.M., Sackesen, C., Erzurum, S., Kalayci, O., 2012. Oxidative Stress and Antioxidant Defense. World Allergy Organ. J. 5, 9–19. https://doi.org/10.1097/WOX.0b013e3182439613

Boswell-Smith, V., Spina, D., Page, C.P., 2006. Phosphodiesterase inhibitors. Br. J. Pharmacol. 147, S252–S257. https://doi.org/10.1038/sj.bjp.0706495

Braidy, N., Grant, R., Adams, S., Brew, B.J., Guillemin, G.J., 2009a. Mechanism for quinolinic acid cytotoxicity in human astrocytes and neurons. Neurotox. Res. 16, 77–86. https://doi.org/10.1007/s12640-009-9051-z

Braidy, N., Grant, R., Adams, S., Brew, B.J., Guillemin, G.J., 2009b. Mechanism for quinolinic acid cytotoxicity in human astrocytes and neurons. Neurotox. Res. 16, 77–86. https://doi.org/10.1007/s12640-009-9051-z

425 Braidy, N., Grant, R., Adams, S., Guillemin, G.J., 2010. Neuroprotective effects of naturally
426 occurring polyphenols on quinolinic acid-induced excitotoxicity in human neurons.
427 FEBS J. 277, 368–382. https://doi.org/10.1111/j.1742-4658.2009.07487.x
428 Cao, X., Zhao, S., Liu, D., Wang, Z., Niu, L., Hou, L., Wang, C., 2011. ROS-Ca2+ is
429 associated with mitochondria permeability transition pore involved in surfactin-
430 induced MCF-7 cells apoptosis. Chem. Biol. Interact. 190, 16–27.
431 https://doi.org/10.1016/j.cbi.2011.01.010
432 Cardinale, A., Fusco, F.R., 2018. Inhibition of phosphodiesterases as a strategy to achieve
433 neuroprotection in Huntington's disease. CNS Neurosci. Ther. 24, 319–328.
434 https://doi.org/10.1111/cns.12834
435 Chandra, R., Aneja, R., Rewal, C., Konduri, R., Dass, S.K., Agarwal, S., 2000. An opium
436 alkaloid-papaverine ameliorates ethanol-induced hepatotoxicity: Diminution of
437 oxidative stress. Indian J. Clin. Biochem. 15, 155–160.
438 https://doi.org/10.1007/BF02883745
439 Chen, Y., Stankovic, R., Cullen, K.M., Meininger, V., Garner, B., Coggan, S., Grant, R.,
440 Brew, B.J., Guillemin, G.J., 2010. The kynurenine pathway and inflammation in
441 amyotrophic lateral sclerosis. Neurotox. Res. 18, 132–142.
442 https://doi.org/10.1007/s12640-009-9129-7
443 Counts, S.E., Nadeem, M., Lad, S.P., Wuu, J., Mufson, E.J., 2006. Differential expression of
444 synaptic proteins in the frontal and temporal cortex of elderly subjects with mild
445 cognitive impairment. J. Neuropathol. Exp. Neurol. 65, 592–601.
446 https://doi.org/10.1097/00005072-200606000-00007
447 D'Amelio, M., Cavallucci, V., Cecconi, F., 2010. Neuronal caspase-3 signaling: not only cell
448 death. Cell Death Differ. 17, 1104–1114. https://doi.org/10.1038/cdd.2009.180
449 Dang, Y., Mu, Y., Wang, K., Xu, K., Yang, J., Zhu, Y., Luo, B., 2016. Papaverine inhibits
450 lipopolysaccharide-induced microglial activation by suppressing NF-κB signaling
451 pathway. Drug Des. Devel. Ther. 10, 851–859. https://doi.org/10.2147/DDDT.S97380
452 Dos Santos, A.A., López-Granero, C., Farina, M., Rocha, J.B.T., Bowman, A.B., Aschner,
453 M., 2018. Oxidative stress, caspase-3 activation and cleavage of ROCK-1 play an
454 essential role in MeHg-induced cell death in primary astroglial cells. Food Chem.
455 Toxicol. Int. J. Publ. Br. Ind. Biol. Res. Assoc. 113, 328–336.
456 https://doi.org/10.1016/j.fct.2018.01.057

457 Fernandez-Marcos, P.J., Auwerx, J., 2011. Regulation of PGC-1α, a nodal regulator of
458 mitochondrial biogenesis1234. Am. J. Clin. Nutr. 93, 884S-890S.
459 https://doi.org/10.3945/ajcn.110.001917
460 García, A.M., Redondo, M., Martinez, A., Gil, C., 2014. Phosphodiesterase 10 inhibitors:
461 new disease modifying drugs for Parkinson's disease? Curr. Med. Chem. 21, 1171–
462 1187. https://doi.org/10.2174/09298673216661312282217 49
463 Giampà, C., Laurenti, D., Anzilotti, S., Bernardi, G., Menniti, F.S., Fusco, F.R., 2010.
464 Inhibition of the Striatal Specific Phosphodiesterase PDE10A Ameliorates Striatal
465 and Cortical Pathology in R6/2 Mouse Model of Huntington's Disease. PLOS ONE 5,
466 e13417. https://doi.org/10.1371/journal.pone.0013417
467 Giralt, A., Saavedra, A., Carretón, O., Arumí, H., Tyebji, S., Alberch, J., Pérez-Navarro, E.,
468 2013. PDE10 inhibition increases GluA1 and CREB phosphorylation and improves
469 spatial and recognition memories in a Huntington's disease mouse model.
470 Hippocampus 23, 684–695. https://doi.org/10.1002/hipo.22128
471 Guillemin, G.J., 2012. Quinolinic acid, the inescapable neurotoxin. FEBS J. 279, 1356–1365.
472 https://doi.org/10.1111/j.1742-4658.2012.08485.x
473 Guillemin, G. J., Brew, B.J., Noonan, C.E., Takikawa, O., Cullen, K.M., 2005. Indoleamine
474 2,3 dioxygenase and quinolinic acid immunoreactivity in Alzheimer's disease
475 hippocampus. Neuropathol. Appl. Neurobiol. 31, 395–404.
476 https://doi.org/10.1111/j.1365-2990.2005.00655.x
477 Guillemin, G.J., Cullen, K.M., Lim, C.K., Smythe, G.A., Garner, B., Kapoor, V., Takikawa,
478 O., Brew, B.J., 2007. Characterization of the kynurenine pathway in human neurons. J.
479 Neurosci. Off. J. Soc. Neurosci. 27, 12884–12892.
480 https://doi.org/10.1523/JNEUROSCI.4101-07.2007
481 Guillemin, Gilles J, Wang, L., Brew, B.J., 2005. Quinolinic acid selectively induces apoptosis
482 of human astrocytes: potential role in AIDS dementia complex. J. Neuroinflammation
483 2, 16. https://doi.org/10.1186/1742-2094-2-16
484 Han, X., Lamshöft, M., Grobe, N., Ren, X., Fist, A.J., Kutchan, T.M., Spiteller, M., Zenk,
485 M.H., 2010. The biosynthesis of papaverine proceeds via (S)-reticuline.
486 Phytochemistry 71, 1305–1312. https://doi.org/10.1016/j.phytochem.2010.04.022
487 Hankir, M.K., Kranz, M., Gnad, T., Weiner, J., Wagner, S., Deuther□Conrad, W., Bronisch,
488 F., Steinhoff, K., Luthardt, J., Klöting, N., Hesse, S., Seibyl, J.P., Sabri, O., Heiker,
489 J.T., Blüher, M., Pfeifer, A., Brust, P., Fenske, W.K., 2016. A novel thermoregulatory

role for PDE10A in mouse and human adipocytes. EMBO Mol. Med. 8, 796–812. https://doi.org/10.15252/emmm.201506085

Harada, A., Suzuki, K., Kimura, H., 2017. TAK-063, a Novel Phosphodiesterase 10A Inhibitor, Protects from Striatal Neurodegeneration and Ameliorates Behavioral Deficits in the R6/2 Mouse Model of Huntington's Disease. J. Pharmacol. Exp. Ther. 360, 75–83. https://doi.org/10.1124/jpet.116.237388

Heckman, P.R.A., van Duinen, M.A., Bollen, E.P.P., Nishi, A., Wennogle, L.P., Blokland, A., Prickaerts, J., 2016. Phosphodiesterase Inhibition and Regulation of Dopaminergic Frontal and Striatal Functioning: Clinical Implications. Int. J. Neuropsychopharmacol. 19. https://doi.org/10.1093/ijnp/pyw030

Huttenlocher, P.R., Dabholkar, A.S., 1997. Regional differences in synaptogenesis in human cerebral cortex. J. Comp. Neurol. 387, 167–178. https://doi.org/10.1002/(sici)1096-9861(19971020)387:2<167::aid-cne1>3.0.co;2-z

Islam, M.T., 2017. Oxidative stress and mitochondrial dysfunction-linked neurodegenerative disorders. Neurol. Res. 39, 73–82. https://doi.org/10.1080/01616412.2016.1251711

Jabaris, S.G.S.L., Sumathy, H., Kumar, R.S., Narayanan, S., Thanikachalam, S., Babu, C.S., 2015. Effects of rolipram and roflumilast, phosphodiesterase-4 inhibitors, on hypertension-induced defects in memory function in rats. Eur. J. Pharmacol. 746, 138–147. https://doi.org/10.1016/j.ejphar.2014.10.039

Jourdi, H., Kabbaj, M., 2013. Acute BDNF Treatment Upregulates GluR1-SAP97 and GluR2-GRIP1 Interactions: Implications for Sustained AMPA Receptor Expression. PLOS ONE 8, e57124. https://doi.org/10.1371/journal.pone.0057124

Jung, J.-S., Shin, J.A., Park, E.-M., Lee, J.-E., Kang, Y.-S., Min, S.-W., Kim, D.-H., Hyun, J.-W., Shin, C.-Y., Kim, H.-S., 2010. Anti-inflammatory mechanism of ginsenoside Rh1 in lipopolysaccharide-stimulated microglia: critical role of the protein kinase A pathway and hemeoxygenase-1 expression. J. Neurochem. 115, 1668–1680. https://doi.org/10.1111/j.1471-4159.2010.07075.x

Kim, J.H., Yi, H.-J., Ko, Y., Kim, Y.-S., Kim, D.-W., Kim, J.-M., 2014. Effectiveness of papaverine cisternal irrigation for cerebral vasospasm after aneurysmal subarachnoid hemorrhage and measurement of biomarkers. Neurol. Sci. Off. J. Ital. Neurol. Soc. Ital. Soc. Clin. Neurophysiol. 35, 715–722. https://doi.org/10.1007/s10072-013-1589-0

Kim, S.M., Chung, M.J., Ha, T.J., Choi, H.N., Jang, S.J., Kim, S.O., Chun, M.H., Do, S.I., Choo, Y.K., Park, Y.I., 2012. Neuroprotective effects of black soybean anthocyanins

524 via inactivation of ASK1-JNK/p38 pathways and mobilization of cellular sialic acids.
525 Life Sci. 90, 874–882. https://doi.org/10.1016/j.lfs.2012.04.025
526 Kowiański, P., Lietzau, G., Czuba, E., Waśkow, M., Steliga, A., Moryś, J., 2018. BDNF: A
527 Key Factor with Multipotent Impact on Brain Signaling and Synaptic Plasticity. Cell.
528 Mol. Neurobiol. 38, 579–593. https://doi.org/10.1007/s10571-017-0510-4
529 Lee, Y.-Y., Park, J.-S., Leem, Y.-H., Park, J.-E., Kim, D.-Y., Choi, Y.-H., Park, E.-M., Kang,
530 J.L., Kim, H.-S., 2019a. The phosphodiesterase 10 inhibitor papaverine exerts anti-
531 inflammatory and neuroprotective effects via the PKA signaling pathway in
532 neuroinflammation and Parkinson's disease mouse models. J. Neuroinflammation 16,
533 246. https://doi.org/10.1186/s12974-019-1649-3
534 Lee, Y.-Y., Park, J.-S., Leem, Y.-H., Park, J.-E., Kim, D.-Y., Choi, Y.-H., Park, E.-M., Kang,
535 J.L., Kim, H.-S., 2019b. The phosphodiesterase 10 inhibitor papaverine exerts anti-
536 inflammatory and neuroprotective effects via the PKA signaling pathway in
537 neuroinflammation and Parkinson's disease mouse models. J. Neuroinflammation 16,
538 246. https://doi.org/10.1186/s12974-019-1649-3
539 Leenders, A.G.M., Sheng, Z.-H., 2005. Modulation of neurotransmitter release by the second
540 messenger-activated protein kinases: Implications for presynaptic plasticity.
541 Pharmacol. Ther. 105, 69–84. https://doi.org/10.1016/j.pharmthera.2004.10.012
542 Lim, C.K., Bilgin, A., Lovejoy, D.B., Tan, V., Bustamante, S., Taylor, B.V., Bessede, A.,
543 Brew, B.J., Guillemin, G.J., 2017. Kynurenine pathway metabolomics predicts and
544 provides mechanistic insight into multiple sclerosis progression. Sci. Rep. 7, 1–9.
545 https://doi.org/10.1038/srep41473
546 Miranda, M., Morici, J.F., Zanoni, M.B., Bekinschtein, P., 2019. Brain-Derived Neurotrophic
547 Factor: A Key Molecule for Memory in the Healthy and the Pathological Brain. Front.
548 Cell. Neurosci. 13. https://doi.org/10.3389/fncel.2019.00363
549 Mishra, J., Kumar, A., 2014. Improvement of mitochondrial function by paliperidone
550 attenuates quinolinic acid-induced behavioural and neurochemical alterations in rats:
551 implications in Huntington's disease. Neurotox. Res. 26, 363–381.
552 https://doi.org/10.1007/s12640-014-9469-9
553 Mizuno, T., Kurotani, T., Komatsu, Y., Kawanokuchi, J., Kato, H., Mitsuma, N., Suzumura,
554 A., 2004. Neuroprotective role of phosphodiesterase inhibitor ibudilast on neuronal
555 cell death induced by activated microglia. Neuropharmacology 46, 404–411.
556 https://doi.org/10.1016/j.neuropharm.2003.09.009

557 Nazir, F.H., Becker, B., Brinkmalm, A., Höglund, K., Sandelius, Å., Bergström, P., Satir,
558 T.M., Öhrfelt, A., Blennow, K., Agholme, L., Zetterberg, H., 2018. Expression and
559 secretion of synaptic proteins during stem cell differentiation to cortical neurons.
560 Neurochem. Int. 121, 38–49. https://doi.org/10.1016/j.neuint.2018.10.014
561 Niccolini, F., Haider, S., Reis Marques, T., Muhlert, N., Tziortzi, A.C., Searle, G.E., Natesan,
562 S., Piccini, P., Kapur, S., Rabiner, E.A., Gunn, R.N., Tabrizi, S.J., Politis, M., 2015.
563 Altered PDE10A expression detectable early before symptomatic onset in
564 Huntington's disease. Brain 138, 3016–3029. https://doi.org/10.1093/brain/awv214
565 Persson, J., Szalisznyó, K., Antoni, G., Wall, A., Fällmar, D., Zora, H., Bodén, R., 2020.
566 Phosphodiesterase 10A levels are related to striatal function in schizophrenia: a
567 combined positron emission tomography and functional magnetic resonance imaging
568 study. Eur. Arch. Psychiatry Clin. Neurosci. 270, 451–459.
569 https://doi.org/10.1007/s00406-019-01021-0
570 Radiske, A., Rossato, J.I., Gonzalez, M.C., Köhler, C.A., Bevilaqua, L.R., Cammarota, M.,
571 2017. BDNF controls object recognition memory reconsolidation. Neurobiol. Learn.
572 Mem., Memory reconsolidation and memory updating 142, 79–84.
573 https://doi.org/10.1016/j.nlm.2017.02.018
574 Rahman, A., Rao, M.S., Khan, K.M., 2018. Intraventricular infusion of quinolinic acid
575 impairs spatial learning and memory in young rats: a novel mechanism of lead-
576 induced neurotoxicity. J. Neuroinflammation 15, 263. https://doi.org/10.1186/s12974-
577 018-1306-2
578 Ren, J.-G., Seth, P., Everett, P., Clish, C.B., Sukhatme, V.P., 2010. Induction of Erythroid
579 Differentiation in Human Erythroleukemia Cells by Depletion of Malic Enzyme 2.
580 PLOS ONE 5, e12520. https://doi.org/10.1371/journal.pone.0012520
581 Rodefer, J.S., Saland, S.K., Eckrich, S.J., 2012. Selective phosphodiesterase inhibitors
582 improve performance on the ED/ID cognitive task in rats. Neuropharmacology 62,
583 1182–1190. https://doi.org/10.1016/j.neuropharm.2011.08.008
584 Roush, E., Harlen, K., Hendrickson, M., Hughes, T.E., 2020. Neurodegenerative Disease and
585 cAMP Signaling Dynamics. Biophys. J. 118, 456a.
586 https://doi.org/10.1016/j.bpj.2019.11.2540
587 Schmidt, C.J., Chapin, D.S., Cianfrogna, J., Corman, M.L., Hajos, M., Harms, J.F., Hoffman,
588 W.E., Lebel, L.A., McCarthy, S.A., Nelson, F.R., Proulx-LaFrance, C., Majchrzak,
589 M.J., Ramirez, A.D., Schmidt, K., Seymour, P.A., Siuciak, J.A., Tingley, F.D.,
590 Williams, R.D., Verhoest, P.R., Menniti, F.S., 2008. Preclinical Characterization of

591 Selective Phosphodiesterase 10A Inhibitors: A New Therapeutic Approach to the
592 Treatment of Schizophrenia. J. Pharmacol. Exp. Ther. 325, 681–690.
593 https://doi.org/10.1124/jpet.107.132910
594 Siuciak, J.A., McCarthy, S.A., Chapin, D.S., Fujiwara, R.A., James, L.C., Williams, R.D.,
595 Stock, J.L., McNeish, J.D., Strick, C.A., Menniti, F.S., Schmidt, C.J., 2006. Genetic
596 deletion of the striatum-enriched phosphodiesterase PDE10A: evidence for altered
597 striatal function. Neuropharmacology 51, 374–385.
598 https://doi.org/10.1016/j.neuropharm.2006.01.012
599 Smith, S.M., Uslaner, J.M., Cox, C.D., Huszar, S.L., Cannon, C.E., Vardigan, J.D., Eddins,
600 D., Toolan, D.M., Kandebo, M., Yao, L., Raheem, I.T., Schreier, J.D., Breslin, M.J.,
601 Coleman, P.J., Renger, J.J., 2013. The novel phosphodiesterase 10A inhibitor THPP-1
602 has antipsychotic-like effects in rat and improves cognition in rat and rhesus monkey.
603 Neuropharmacology 64, 215–223. https://doi.org/10.1016/j.neuropharm.2012.06.013
604 Steffan, J.S., Kazantsev, A., Spasic-Boskovic, O., Greenwald, M., Zhu, Y.-Z., Gohler, H.,
605 Wanker, E.E., Bates, G.P., Housman, D.E., Thompson, L.M., 2000. The Huntington's
606 disease protein interacts with p53 and CREB-binding protein and represses
607 transcription. Proc. Natl. Acad. Sci. 97, 6763–6768.
608 https://doi.org/10.1073/pnas.100110097
609 Sumathi, T., Vedagiri, A., Ramachandran, S., Purushothaman, B., 2018. Quinolinic Acid-
610 Induced Huntington Disease-Like Symptoms Mitigated by Potent Free Radical
611 Scavenger Edaravone—a Pilot Study on Neurobehavioral, Biochemical, and
612 Histological Approach in Male Wistar Rats. J. Mol. Neurosci. 66, 322–341.
613 https://doi.org/10.1007/s12031-018-1168-1
614 Sundaram, G., Brew, B.J., Jones, S.P., Adams, S., Lim, C.K., Guillemin, G.J., 2014.
615 Quinolinic acid toxicity on oligodendroglial cells: relevance for multiple sclerosis and
616 therapeutic strategies. J. Neuroinflammation 11, 204. https://doi.org/10.1186/s12974-
617 014-0204-5
618 Suzumura, A., Ito, A., Yoshikawa, M., Sawada, M., 1999. Ibudilast suppresses TNFalpha
619 production by glial cells functioning mainly as type III phosphodiesterase inhibitor in
620 the CNS. Brain Res. 837, 203–212. https://doi.org/10.1016/s0006-8993(99)01666-2
621 Valtschanoff, J.G., Burette, A., Davare, M.A., Leonard, A.S., Hell, J.W., Weinberg, R.J.,
622 2000. SAP97 concentrates at the postsynaptic density in cerebral cortex. Eur. J.
623 Neurosci. 12, 3605–3614. https://doi.org/10.1046/j.1460-9568.2000.00256.x

624 Wang, H., Xu, J., Lazarovici, P., Quirion, R., Zheng, W., 2018. cAMP Response Element-
625 Binding Protein (CREB): A Possible Signaling Molecule Link in the Pathophysiology
626 of Schizophrenia. Front. Mol. Neurosci. 11. https://doi.org/10.3389/fnmol.2018.00255
627 Wilson, R.F., White, C.W., 1986. Intracoronary papaverine: an ideal coronary vasodilator for
628 studies of the coronary circulation in conscious humans. Circulation 73, 444–451.
629 https://doi.org/10.1161/01.cir.73.3.444
630 Wu, Y., Chen, M., Jiang, J., 2019. Mitochondrial dysfunction in neurodegenerative diseases
631 and drug targets via apoptotic signaling. Mitochondrion 49, 35–45.
632 https://doi.org/10.1016/j.mito.2019.07.003
633 Yurtsever Kum, N., Yilmaz, Y.F., Gurgen, S.G., Kum, R.O., Ozcan, M., Unal, A., 2018.
634 Effects of Parenteral Papaverine and Piracetam Administration on Cochlea Following
635 Acoustic Trauma. Noise Health 20, 47–52. https://doi.org/10.4103/nah.NAH_31_17
636 Zinger, A., Barcia, C., Herrero, M.T., Guillemin, G.J., 2011. The Involvement of
637 Neuroinflammation and Kynurenine Pathway in Parkinson's Disease [WWW
638 Document]. Park. Dis. https://doi.org/10.4061/2011/716859
639

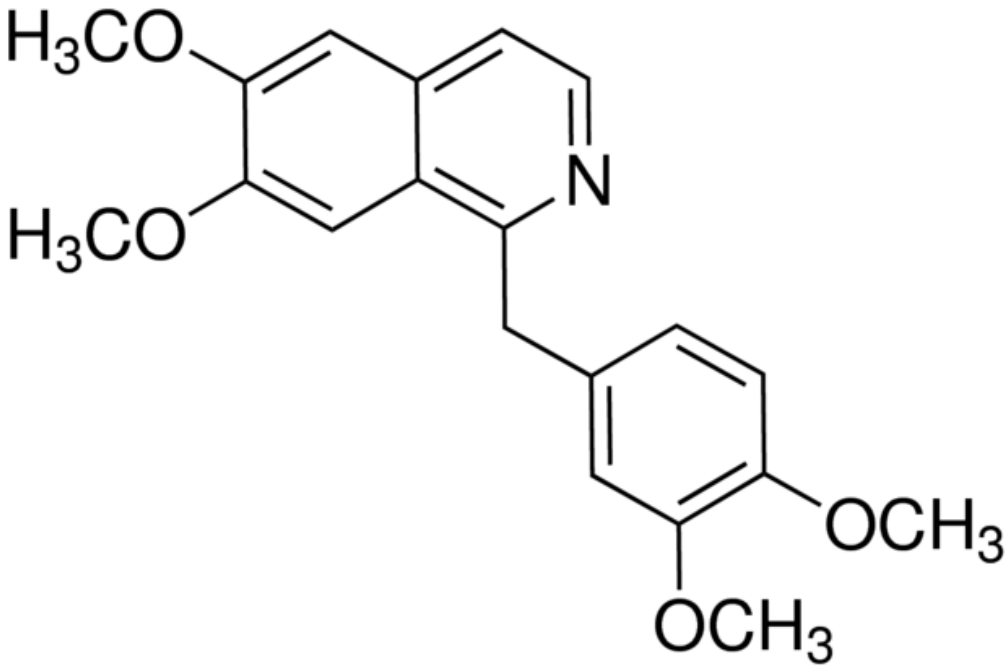

Figure 1: Chemical structure of Papaverine drawn with ChemBioDraw Ultra 12.

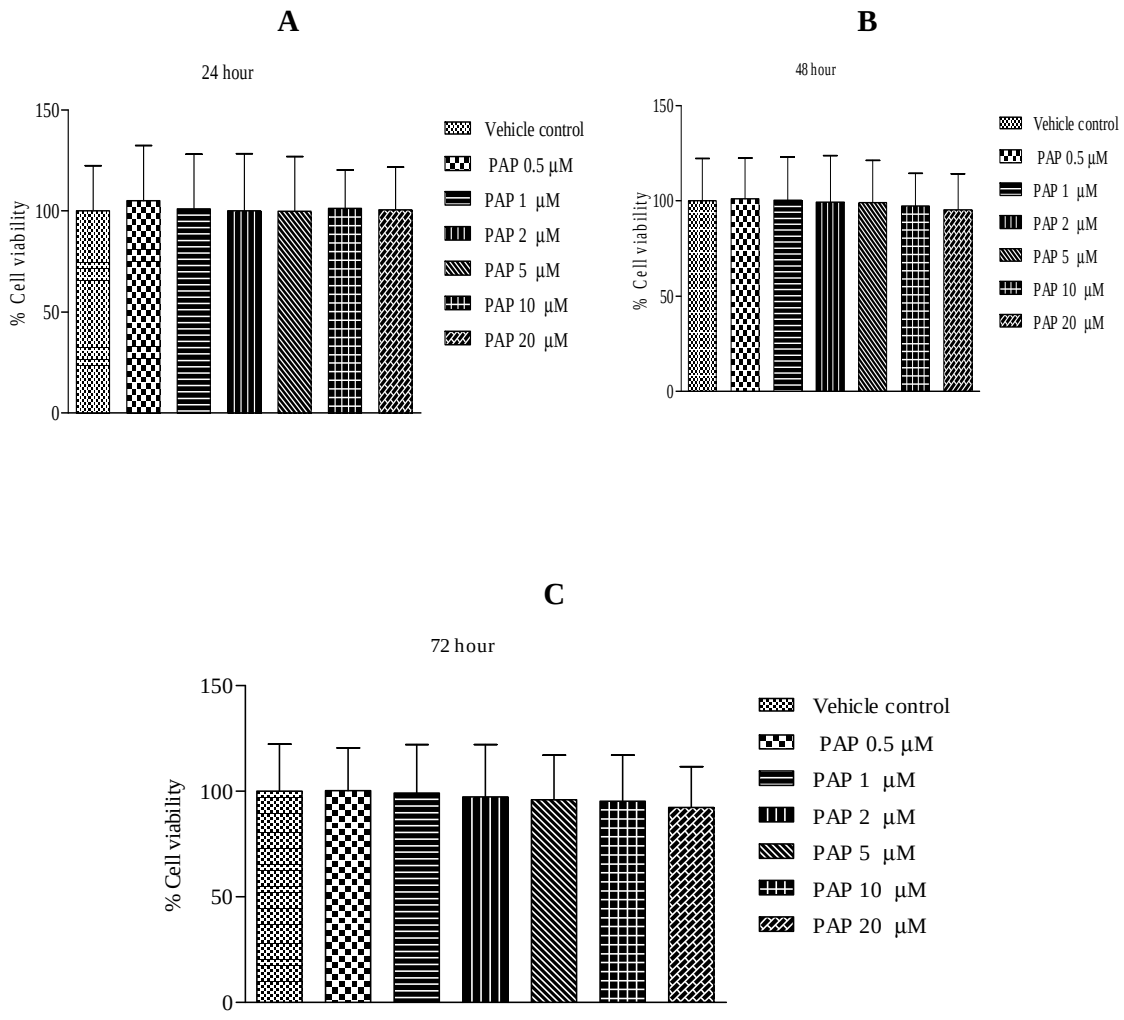

Figure 2: Papaverine did not show toxic effects at the tested concentration in human cortical neurons. (A) Human cortical neurons were treated with various concentrations of PAP and assessed for cell viability at 24 (A), 48 (B) and 72 h (C) using MTS solution.

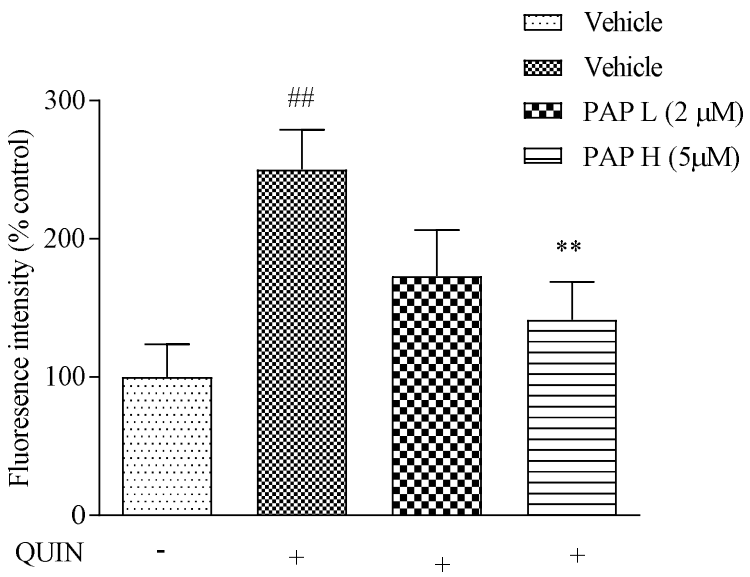

Figure 3: Papaverine reduces QUIN-induced ROS production in human neurons. Neurons were pre-treated with PAP (2μM & 5 μM) for 24 hours, followed by 48-hour exposure with QUIN (2μM). Data are presented as mean ± SEM (n = 3) and represent three independent experiments. ## denotes $p < 0.01$ vs vehicle, ** denotes $p < 0.01$ vs QUIN exposed neurons

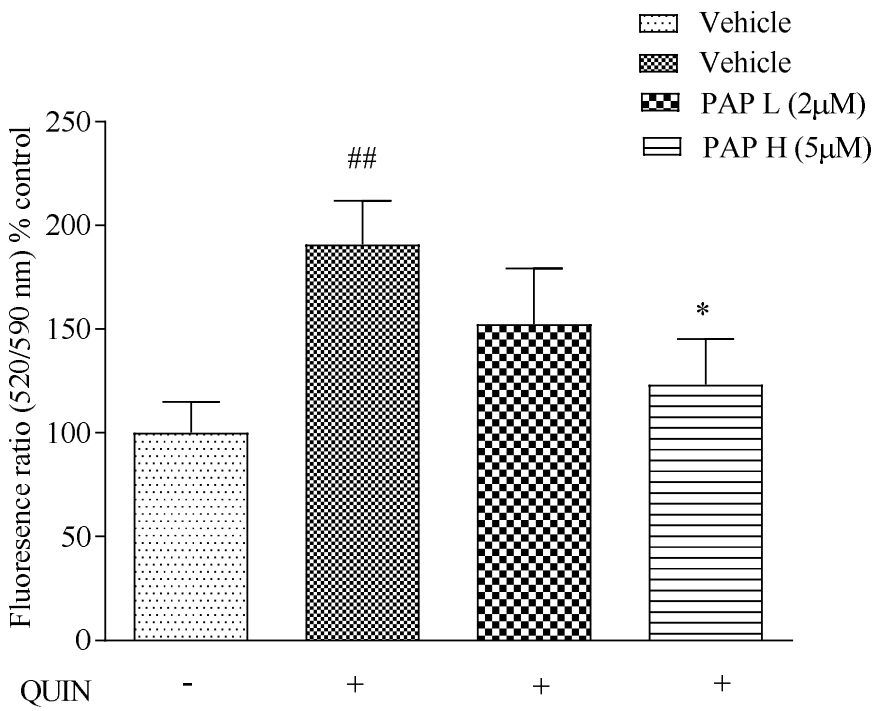

Figure 4: Papaverine restores mitochondrial membrane potential in QUIN exposed human cortical neurons. Neurons were pretreated with PAP (2μM & 5 μM) for 24 hours, followed by 48-hour exposure with QUIN (2μM). Neurons were incubated with JC-10 (30 μM) for 20 min. Data are presented as mean ± SEM (n = 3) and represent three independent experiments. ## denotes $p < 0.01$ vs vehicle, * denotes $p < 0.05$ vs QUIN exposed neurons

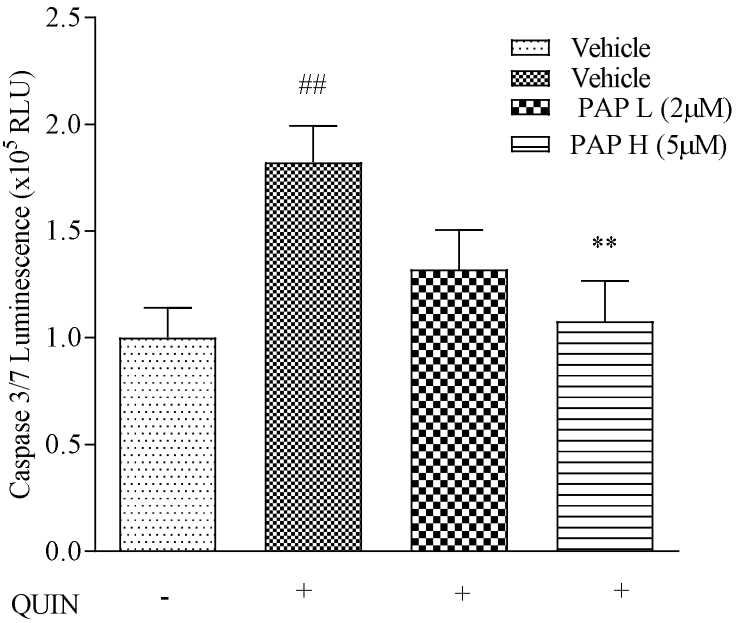

Figure 5: Papaverine decreases Caspase 3/7 activity in QUIN exposed human neurons. Neurons were pre-treated with PAP (2μM & 5 μM) for 24 hours, followed by 48-hour exposure with QUIN (2μM). Caspase 3/7 activity was assessed using ApoTox-Glo Triplex Assay kit (Promega, Madison, WI, USA). Data are presented as mean ± SEM (n = 3) and represent three independent experiments. $^{\#\#}$ denotes $p< 0.01$ vs vehicle, **denotes $p< 0.01$ vs QUIN exposed neurons

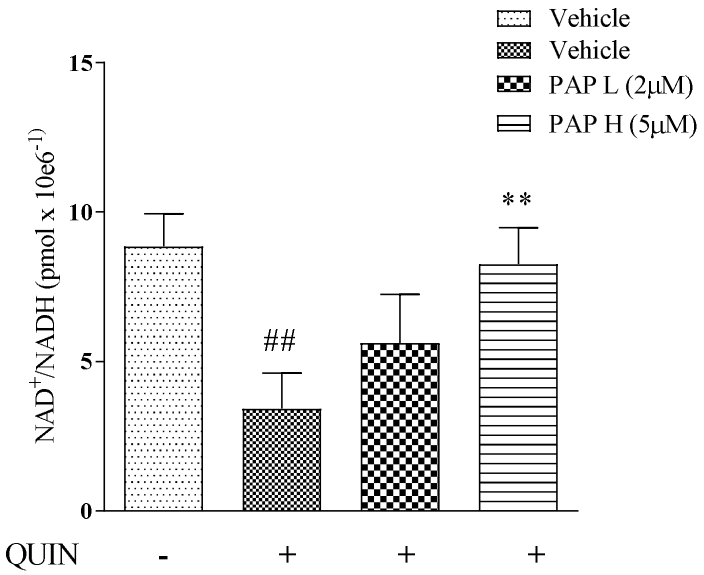

Figure 6: Papaverine increases NAD$^+$/NADH levels in QUIN exposed human neurons. Neurons were pre-treated with PAP (2 μM & 5 μM) for 24 hours, followed by 48-hour exposure with QUIN (2μM). NAD$^+$/NADH concentration were measured in accordance with the manufacturer's instruction (Abcam, Inc., Cambridge, MA, USA). Data are presented as mean ± SEM (n = 3) and represent three independent experiments. $^{\#\#}$ denotes $p< 0.01$ vs vehicle, ** denotes $p< 0.01$ vs QUIN exposed neurons

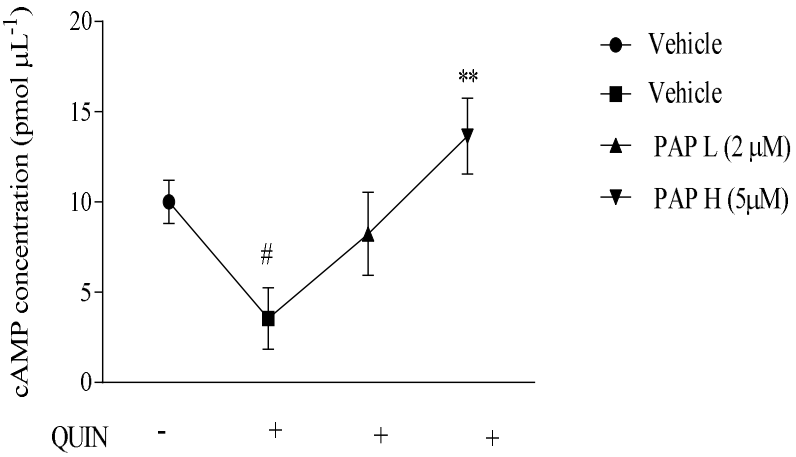

Figure 6: Effect of PAP on cAMP concentration in QUIN exposed human neurons

Pre-treatment with PAP increased cAMP concentration in QUIN exposed human neurons. Data are presented as mean ± SEM (n = 3) and represent three independent experiments. #denotes $p < 0.05$ vs vehicle, **denotes $p < 0.01$ vs QUIN exposed neurons

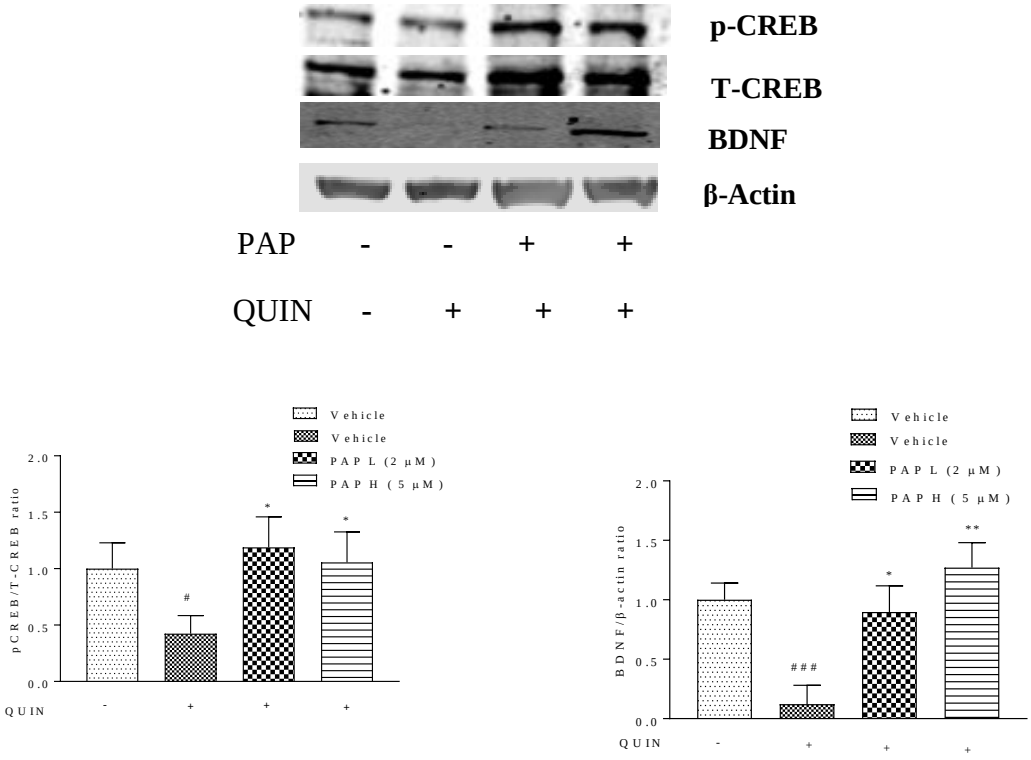

Figure 7: PAP upregulates the expression of CREB and BDNF in QUIN exposed neurons.

Neurons were pre-treated with PAP (2µM & 5 µM) for 24 hours, followed by 48-hour exposure with QUIN (2µM). (A) Quantification of pCREB/T-CREB. (B) Quantification of BDNF/ β-actin. Data are presented as mean ± SEM (n = 3) and represent three independent experiments. $^{\#}$ denotes $p< 0.05$, $^{\#\#\#}$denotes $p< 0.001$ vs vehicle, * denotes $p< 0.05$, ** denotes $p< 0.01$ vs QUIN exposed neurons

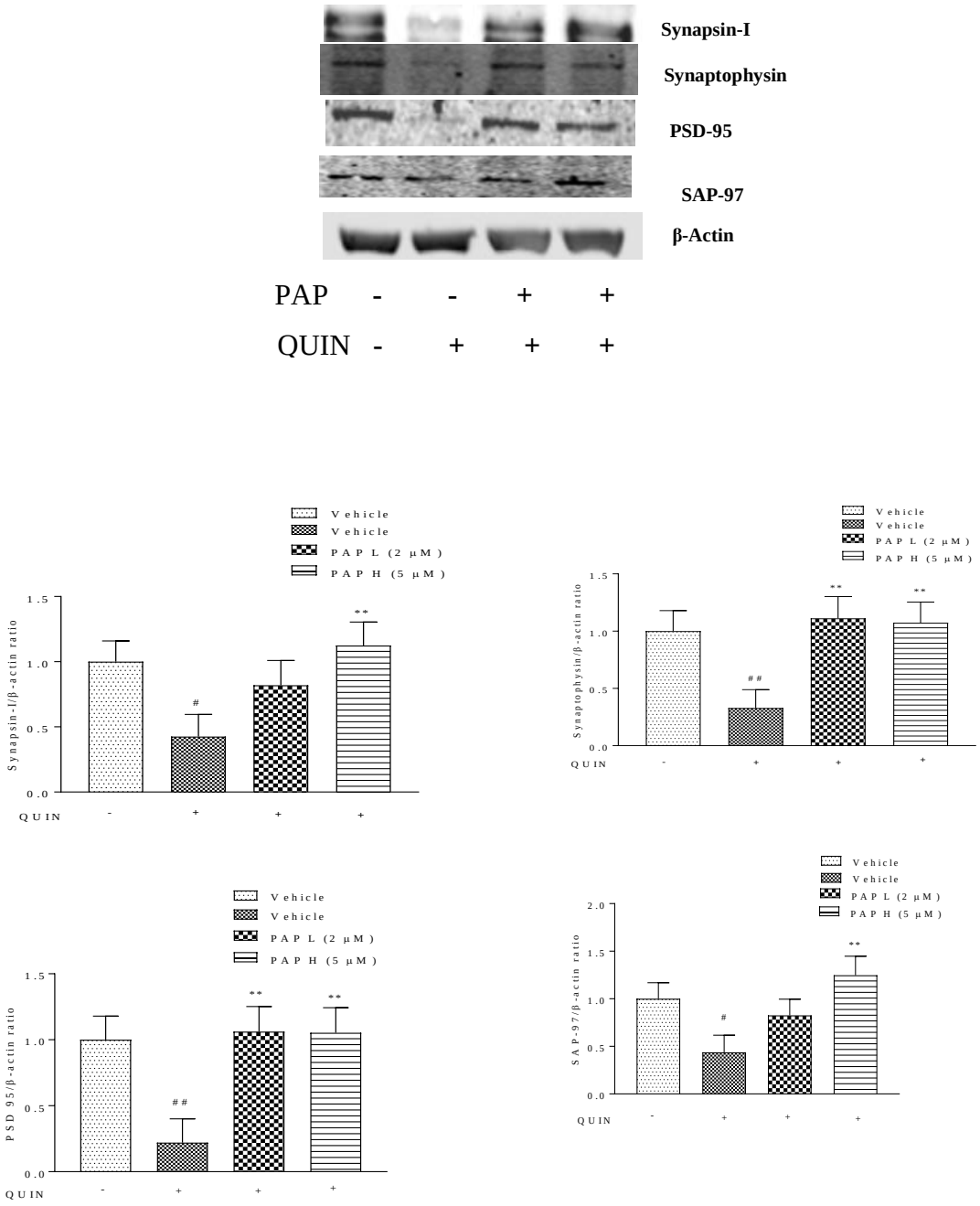

Figure 9: Papaverine increased the expression of Presynaptic and postsynaptic proteins in QUIN exposed neurons. Neurons were pre-treated with PAP (2µM & 5 µM) for 24 hours, followed by 48-hour exposure with QUIN (2µM). (A) Quantification of Synapsin-I-97/β-actin. (B) Quantification of Synaptophysin/ β-actin (C) Quantification of PSD-95/ β-actin (D) Quantification of SAP-97/ β-actin. Data are presented as mean ± SEM (n = 3) and represent three independent experiments. $^{\#}$ denotes $p< 0.05$, $^{\#\#}$denotes $p< 0.01$ vs vehicle, ** denotes $p< 0.01$ vs QUIN exposed neurons

Quinolinic Acid Intoxication

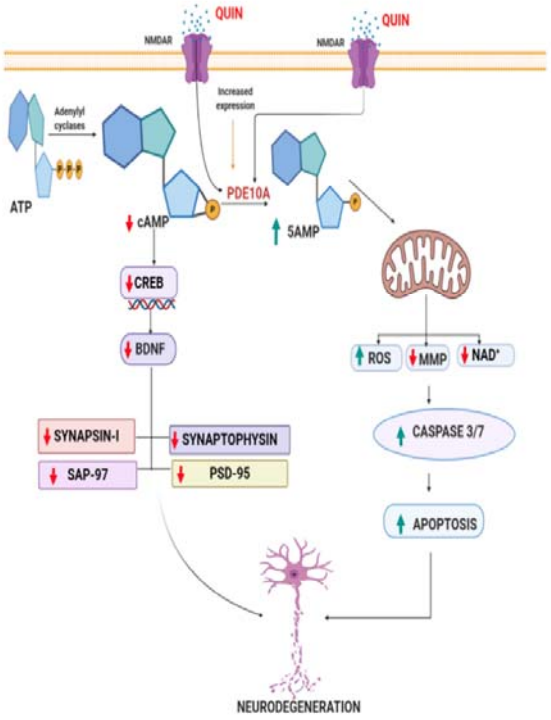

Papaverine Pre-treated + Quinolinic acid Intoxication